

## Observation of the Domain Structures in Soft Magnetic $(\text{Fe}_{97}\text{Al}_3)_{85}\text{N}_{15}/\text{Al}_2\text{O}_3$ Multilayers

T. Stobiecki\* and M. Zoladz

*Department of Electronics, University of Mining and Metallurgy, 30-059 Krakow, Poland*

(Received 10 December 2002)

The longitudinal magneto-optical Kerr effect was used to analyse magnetic domains in soft magnetic  $(\text{Fe}_{97}\text{Al}_3)_{85}\text{N}_{15}/\text{Al}_2\text{O}_3$  multilayers in order to get microscopic understanding of interlayer exchange coupling. The measuring system consists of a Kerr microscope, a CCIR camera (with an 8-bit framegrabber), 16 bit digital camera and computer system for real-time image processing and to control external magnetic field and cameras. The strength of ferromagnetic (FM) coupling as a function of the spacer thickness of  $\text{Al}_2\text{O}_3$  was investigated. It was found that strong FM-coupling, strong uniaxial anisotropy and coherent rotation of the magnetization have been observed for the spacer thickness in the range of  $0.2 \text{ nm} \leq t \leq 1 \text{ nm}$ , however, weak FM-coupling, patch domains and  $360^\circ$ -walls occur for the spacer thickness of  $t = 2.5 \text{ nm}$ . At a spacer thickness of  $t \geq 5 \text{ nm}$  transition takes place from weak FM-coupling to the decoupled state where complex interlayer interactions and different types of the domain walls were observed.

**Key words :** magnetic domains and walls of multilayers, Kerr microscope, real-time image processing, soft magnetic properties of multilayers.

### 1. Introduction

The ability to observe and measure domain structure is very important for understanding and optimising magnetic properties of new magnetic recording materials. For this purpose magneto-optical Kerr effect is very useful and is the recommended method for observation of magnetic domains in multilayers, with the thickness of bilayer smaller than 30 nm (due to exponential decay of light intensity), because it delivers information of interlayer exchange coupling, at different depths of sample thickness [1].

Iron nitride alloy films prepared in the form of laminated  $(\text{Fe}_{97}\text{Al}_3)_{85}\text{N}_{15}/\text{Al}_2\text{O}_3$  multilayers are very promising new magnetic materials for poles and shields in ultra high density thin film heads because of their excellent soft magnetic properties and high saturation magnetization [2]. Nitrogen is usually introduced into iron to improve material properties like hardness, wear and corrosion resistance or to modify magnetic properties. The addition of nitrogen reduces the grain size, thereby making multilayers magnetically soft, and enhances the local magnetic

moments by changing the distances of the interacting moments while an alloying element as Al is thought to increase thermal stability. The  $\text{Al}_2\text{O}_3$  spacers with optimal thickness enhance the ferromagnetic coupling between ferromagnetic  $(\text{Fe}_{97}\text{Al}_3)_{85}\text{N}_{15}$  sublayers which leads to small dispersion of magnetization and rapid decrease of coercive field. The present work concerns the ferromagnetic (FM) coupling effect as a function of the thickness of  $\text{Al}_2\text{O}_3$  spacers by analysis of the magnetic domain structure with digitally enhanced Kerr microscopy.

### 2. Experimental

#### 2.1. Kerr microscope

Due to small Kerr rotation angle in the longitudinal Kerr mode (against the polar mode), domain images obtained directly from Kerr microscope contain very large non-magnetic background which makes the interpretation difficult. Using digital image processing some of non-magnetic contributions can be eliminated. However, the real-time domain structure observation is always preferred. For this purpose software and hardware based on a personal computer (PC) are designed [3].

The measuring system (Fig. 1a and b) consists of a Kerr microscope, a CCIR camera with an 8-bit framegrabber

\*Corresponding author: Tel: (+48 12) 617 2596; Fax: (+48 12) 617 3550, e-mail: stobiecki@uci.agh.edu.pl

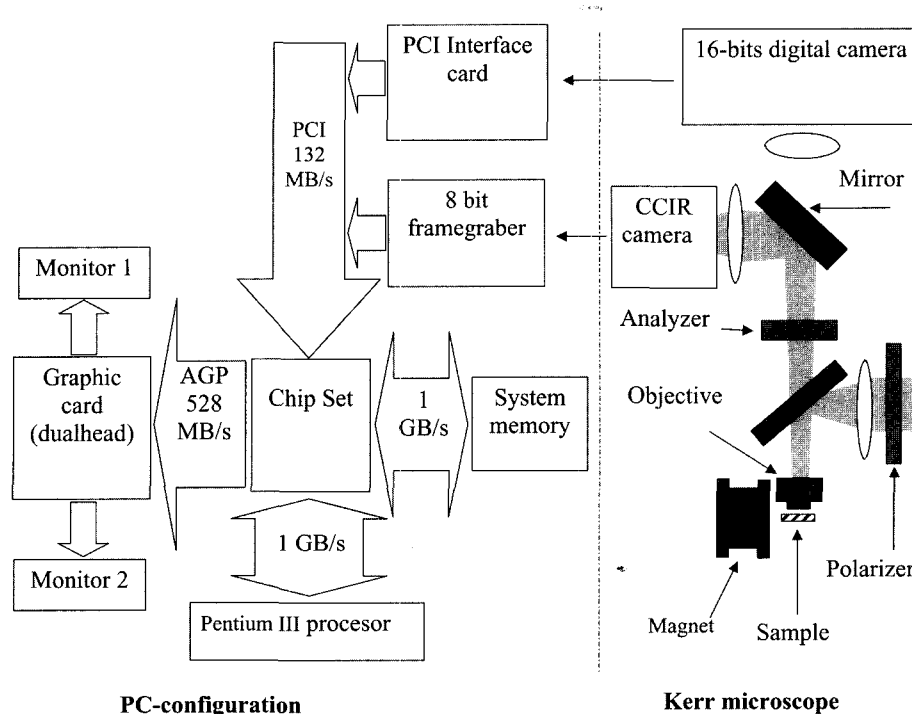


Fig. 1. (a) PC- configuration; (b) arrangement of Kerr microscope.

( $768 \times 576$  pixels and 25 frames per second), a 16 bit digital camera ( $784 \times 520$  pixels and 2 frames per second), a PC equipped with Pentium III 750 MHz processor and AGP *dualhead* graphic card, two monitors and a bipolar power supply for an electromagnet. The cameras and power supply are all controlled by computer. The program is written in C++, working under *Windows operation* system and uses libraries: *Microsoft Foundation Class* (MFC) which cooperates with operating system, *Direct X* which involves direct access to graphic card memory, *Daisy* which cooperates with 8-bit frame grabber and a set of functions for digital camera control. For 8-bit pictures processing the background subtractions with dynamic false palette and median filter have been used [3].

The system and program for real-time magnetic domain observation have been tested in the configuration of polar and longitudinal Kerr effect on different samples: Fe-Tb sputtered multilayers [4], Fe-Au MBE deposited superlattices [5], and amorphous ribbons. At the beginning a CCIR camera with 8-bit framegrabber (25 fps) was used to adjust the optics and make the magnetic domain contrast visible (Fig. 1b). Next the mirror (Fig. 1b) was taken away and pictures were detected by a digital camera. As the digital camera allows long time integration and a high dynamic range the resulting image was characterized by more degrees of gray levels and improved signal-to-noise ratio. Further, the normalization compensates the

inhomogeneity of the Kerr signal which can lead to a big improvement of the image quality.

### 3. Results and Discussion

#### 3.1. Samples

The RF sputtering technique and Si substrates buffered by 100 nm  $\text{Al}_2\text{O}_3$  were used for deposition of  $[(\text{Fe}_{97}\text{Al}_3)_{85}\text{N}_{15}/\text{Al}_2\text{O}_3] \times 16$  multilayers in Ar- $\text{N}_2$  gas mixture. The FM-sublayers  $(\text{Fe}_{97}\text{Al}_3)_{85}\text{N}_{15}$  had a constant thickness of 26 nm and the thickness of the  $\text{Al}_2\text{O}_3$  spacers was varied from 0.2 to 100 nm. A magnetic field (2 kA/m) was applied during deposition to induce uniaxial anisotropy. The recently published results of phase analysis show predominantly the  $\alpha$ -Fe and the  $\gamma'$ - $\text{Fe}_4\text{N}$  phase, regardless of  $\text{Al}_2\text{O}_3$  thickness [6]. The coercivity ( $H_C$ ) of MI's is very small (40 A/m) and increases slightly with increasing thickness of  $\text{Al}_2\text{O}_3$  (Fig. 2). The uniaxial anisotropy field ( $H_k$ ) increases from about  $H_k = 480$  A/m at  $\text{Al}_2\text{O}_3$  thickness of 0.22 nm to a maximum ( $H_k = 640$  A/m) for 1 nm thick  $\text{Al}_2\text{O}_3$ . Above 10 nm thickness of  $\text{Al}_2\text{O}_3$  the uniaxial anisotropy field is approximately constant ( $H_k \approx 480$  A/m) (Fig. 2). The angular dispersion ( $\alpha$ ) of easy axis is small ( $\alpha \approx 0.8^\circ$ ) in the range from 0.22 nm to 2 nm and then increases achieving  $\alpha = 3.8^\circ$  for 100 nm (Fig. 2). The saturation of magnetization is constant ( $J_S \approx 1.6$  T) and is independent of thickness of  $\text{Al}_2\text{O}_3$ .

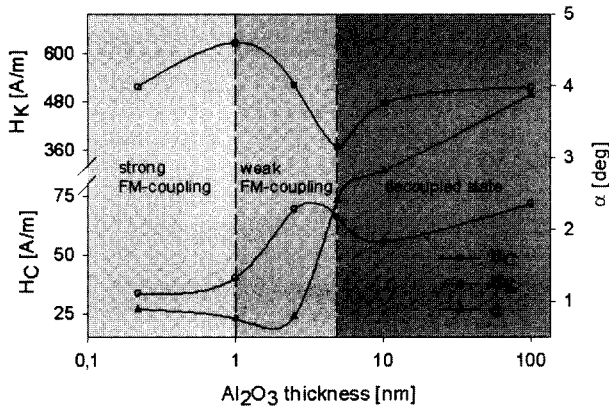


**Fig. 2.** Coercivity ( $H_C$ ), anisotropy ( $H_K$ ) fields and angular dispersion ( $\alpha$ ) vs. thickness of  $Al_2O_3$  spacer in multilayers of  $[(Fe_{97}Al_3)_{85}N_{15} (26 \text{ nm})/Al_2O_3(t)] \times 16$ .

**3.2. Analysis of the domain structure**

Depending on the thickness of  $Al_2O_3$  different stages of FM-coupling were observed. For the thickness of 0.22 nm and 1 nm the strong FM-coupling was observed, which led to very soft magnetic samples, closed and linear hysteresis in the hard direction, very small dispersion of magnetization ( $\alpha=0.7^\circ$ ) and rectangular hysteresis loop in easy direction with  $H_C \approx 40 \text{ A/m}$ . In consequence infinitely long domains develop, which coherently rotate (Fig. 3) in external magnetic field ( $H < 0.5 H_K$ ). During magnetizing along the hard direction in the field  $H > 0.5 H_K$ , parallel domain stripes and weak ripple structure from the top and bottom layer are observed (Fig. 4). Increase of the spacer thickness above 2.5 nm leads to weakening of the FM-coupling so that  $360^\circ$ -walls are

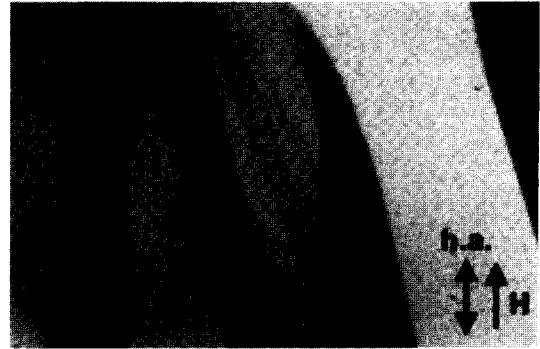


**Fig. 4.** The ripple structure for  $t = 0.22 \text{ nm}$  of  $Al_2O_3$ . Picture size  $265 \times 179 \mu\text{m}$ .

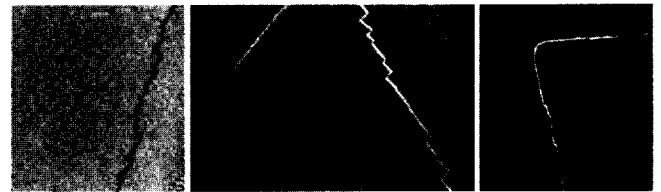


**Fig. 5.**  $360^\circ$ -walls for  $t = 2.5 \text{ nm}$  of  $Al_2O_3$ . The zig-zag nature is due to energy minimum. Middle picture size  $265 \times 179 \mu\text{m}$ , side pictures size  $166 \times 179 \mu\text{m}$ .

formed (Fig. 5). The  $360^\circ$ -wall may be generated if a  $180^\circ$ -wall sweeps over a pinhole, that is able to trap the Bloch line [7, 8]. In a narrow angular range around the hard axes an irregular patch domain pattern develops (Fig. 6a). This image can be explained qualitatively by reducing (in external field) the transversal component of magnetization as indicated in the sketch (Fig. 6b). The transition from weak FM-coupling to decoupled state was

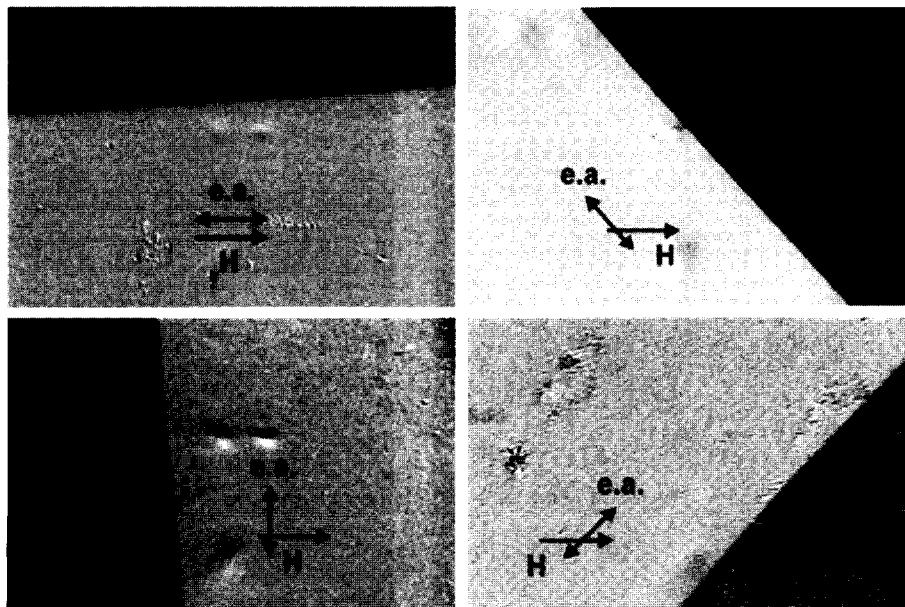


**Fig. 3.** Infinitely long domains rotating in a field  $H = 0.13 H_K$  for  $t = 0.22 \text{ nm}$  of  $Al_2O_3$ . Picture size  $275 \times 179 \mu\text{m}$ .

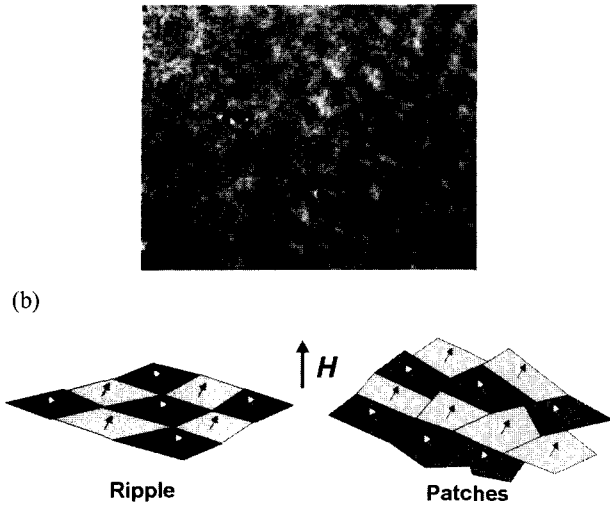
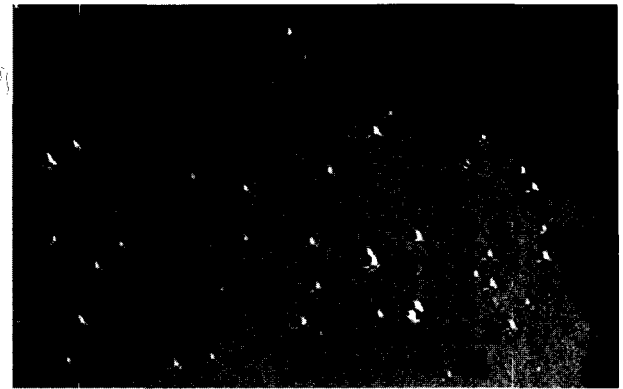
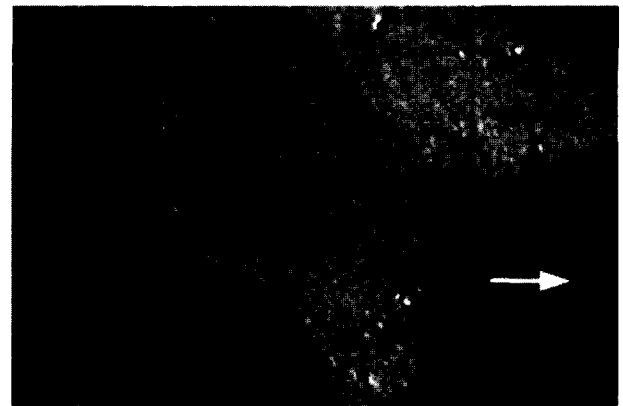


**Fig. 6.** (a) Patch domain patterns for  $t = 2.5$  nm of  $\text{Al}_2\text{O}_3$ , in field  $H = 0.91 H_K$ . Picture size  $65 \times 45 \mu\text{m}$ . (b) Ripple and patche images in MI's. Coupling by patches is weaker than by ripples because magnetic moments (indicated by white and black arrows, on the top and bottom layers, respectively) are not oriented parallel.

investigated in 4.9 nm thick spacers of  $\text{Al}_2\text{O}_3$ . The patch domains effect in this case is very strong, therefore it is observed not only in the hard direction but also in between the hard and easy axis and additionally with  $360^\circ$ - and  $180^\circ$ -symmetric Néel walls [9] (Fig. 7). The strong influence of stray fields, in the case of very thick spacers ( $t = 10$  nm), leads to irregular domains (Fig. 8a) and arrangements of  $90^\circ$ -domains when the sample is magnetized in easy direction (Fig. 8b).



(a)



(b)

**Fig. 8.** (a) Irregular domain magnetized along the easy direction for  $t = 10$  nm of  $\text{Al}_2\text{O}_3$ . Picture size  $265 \times 179 \mu\text{m}$ . (b) arrangement of  $90^\circ$ -domains in the remanent state, for  $t = 4.9$  nm  $\text{Al}_2\text{O}_3$ . Picture size  $265 \times 179 \mu\text{m}$ .

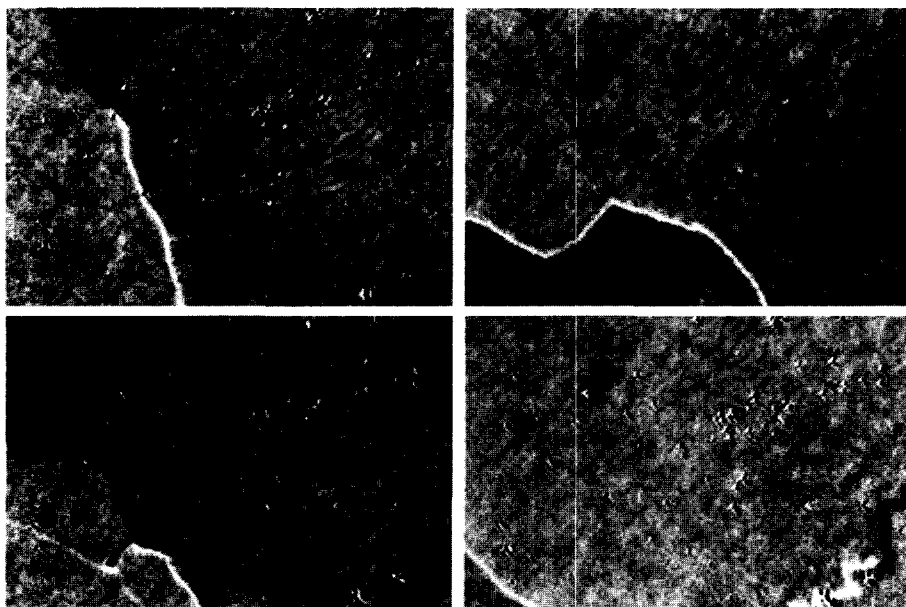


**Fig. 7.**  $360^\circ$ - and  $180^\circ$ -symmetric Néel walls for  $t = 4.9$  nm of  $\text{Al}_2\text{O}_3$ .  $360^\circ$ -wall separates equal contrast areas; a  $180^\circ$ -symmetric Néel wall is present when opposite contrast is seen. Pictures size  $265 \times 179 \mu\text{m}$ .

#### 4. Conclusion

On the basis of magnetic domain analysis we conclude that strong FM-coupling, strong uniaxial anisotropy, very small dispersion of easy axis and coherent rotation of magnetization have been observed for the spacer thickness in the range of  $0.22 \text{ nm} \leq t \leq 1 \text{ nm}$ . Weak FM-coupling,  $360^\circ$ -walls and patch domain patterns (in hard direction) occur for spacer thickness of  $t = 2.5 \text{ nm}$ . The thickness of  $t = 4.9 \text{ nm}$  is characteristic of the transition from weak FM-coupling to the decoupled state where complex interlayer interactions and different domain walls ( $360^\circ$ - and  $180^\circ$ -symmetric Néel) have been observed. A totally decoupled state occurs for  $t > 10 \text{ nm}$  which leads to irregular domains in easy direction due to influence of the stray fields. Finally we conclude that multilayers of  $(\text{Fe}_{97}\text{Al}_3)_{85}\text{N}_{15}$  (26 nm)/ $\text{Al}_2\text{O}_3(t)$  with  $t \approx 1 \text{ nm}$  are very promising as novel material for high density thin film recording heads.

#### References

- [1] R. Schäfer, R. Urban, D. Ullmann, H. L. Meyerheim, B. Heinrich, L. Schultz, and J. Kirschner, *Phys. Rev. B* **65**, 144405 (2002).
- [2] W. Maass, B. Ocker, H. Rohrmann, and R. Mattheis, *J. Magn. Magn. Soc. Japan*, **23**, 249 (1999).
- [3] M. Zoladz, S. Knappmann, M. Otto, K. Röhl, and T. Stobiecki, *Phys. Stat. Sol. (a)* **189**, 791 (2002).
- [4] S. Knappmann, K. Röhl, and F. Stobiecki, *Acta Physica Pol A* **97**, 475 (2000).
- [5] T. Slezak, W. Karas, K. Krop, M. Kubik, D. Wilgocka-Slezak, N. Spiridis, and J. Korecki, *J. Magn. Magn. Mat.* **240**, 362 (2002).
- [6] T. Stobiecki, M. Kopcewicz, W. Powroznik, E. Kusior, P. Wisniowski, W. Maass, B. Ocker, and H. Rohrmann, *J. Magn. Magn. Mat.* **240**, 448 (2002).
- [7] L. J. Heydreman, H. Niedoba, H. O. Gupta, and I. B. Puchalska, *J. Magn. Magn. Mat.* **96**, 125 (1991).
- [8] E. Sanneck, M. Ruehring, and A. Hubert, *IEEE Trans. Magn.* **29**, 2500 (1993).
- [9] A. Hubert and R. Schäfer, *Magnetic Domains*, Springer Berlin (1998) pp. 487-499.